Fracture strength of drilled wafers: study of the stress concentration factor and determination of the Weibull distribution of the fracture stress

J. Barredo[1], C. Alarcón[2] and S. Gómez-Lera[3]

[1]*Centre for Modelling in Mechanical Engineering (CEMIM-F2I2), Madrid, Spain*
[2]*Department of Materials Engineering, UPM, Madrid, Spain*
[3]*Department of Structural Mechanics and Industrial Constructions, UPM, Madrid, Spain*

Abstract

In the photovoltaic field, the back contact solar cells technology has appeared as an alternative to the traditional silicon modules. This new type of cells places both positive and negative contacts on the back side of the cells maximizing the exposed surface to the light and making easier the interconnection of the cells in the module. The Emitter Wrap-Through solar cell structure presents thousands of tiny holes to wrap the emitter from the front surface to the rear surface. These holes are made in a first step over the silicon wafers by means of a laser drilling process. This step is quite harmful from a mechanical point of view since holes act as stress concentrators leading to a reduction in the strength of these wafers.

This paper presents the results of the strength characterization of drilled wafers. The study is carried out testing the samples with the ring on ring device. Finite Element models are developed to simulate the tests. The stress concentration factor of the drilled wafers under this load conditions is determined from the FE analysis. Moreover, the material strength is characterized fitting the fracture stress of the samples to a three-parameter Weibull cumulative distribution function. The parameters obtained are compared with the ones obtained in the analysis of a set of samples without holes to validate the method employed for the study of the strength of silicon drilled wafers.

1 Introduction

There is an increasing commercial and scientific interest in back-contact silicon solar cells due to the special features that make them very attractive in the photovoltaic industry. The back contact structure reduces the grid obscuration losses as well as the module assembly cost due to a simpler geometry placing both positive and negative polarity contacts on the back side of the wafer (Gee [1]).

There are different types of back-contact cells on the market like Metal Wrap-Through (MWT), Emitter Wrap-Through (EWT) or Transistor Wrap-Through (TWT). While MWT and EWT cells have holes of different size and distribution to take the electrons to the back side of

the cell, TWT cells have grooves to improve the transistor effect. Some steps of the manufacturing processes of these cells are quite harmful with regard to the mechanical strength. Hence, studies concerning the mechanical influence of these critical steps have become popular last years (Barredo [2], Schoenfelder [3], Cereceda [4]).

This study is focused on the structure of EWT cells that usually presents thousands of tiny holes whereas MWT cells have fewer but bigger ones. It's quite common in the industry to employ EWT solar cells with approximately 100 holes per square centimetre. These holes act as stress concentrators reducing the strength of the silicon wafers significantly (Bagdahn [5]) and, therefore, increasing the breakage ratio in the EWT cell production line. This ratio is critical for the PV industry (Koepge [6]) as a means of achieving a better understanding of the failure mechanism and subsequently reducing it.

Traditional mechanical design for ductile materials calculates the maximum local stress, σ_{loc}, around a hole by multiplying the gross stress, σ_{gross}, by a stress concentration factor K_{tg}. The maximum local stress is compared with the strength of the material to determine if local plastic deformation will occur. There exists a wide array of literature (Peterson [7]) about the values of K_t depending on the load conditions.

This approach is not valid for brittle materials (Bagdahn [5]) because of the strength dependence on the size of the loaded area or volume. A stress concentration is a small area or volume subjected to high stresses and, therefore, there's less chance to find there a critical flaw leading the failure. Usually, the Weibull statistic, based on the weakest link theory, is employed to characterize the strength of mono-crystalline silicon. In this study, a stress concentration factor, for a biaxial stress state, of drilled silicon wafers is estimated by finite element models and the result is compared with the one found in the literature. Moreover, from these results, the material strength curve is determined and it's compared with the one obtained with a set of wafers without holes.

2 Material and sample preparation

Two sets of silicon wafers have been prepared for the study. The first set represents the physical structure of a commercial EWT solar cell. First of all, the wafers have been chemically etched to remove any possible surface damage from wire-sawing (Barredo [8]). After that, the wafers have been drilled by a laser process following a EWT pattern. The pattern consists of a matrix of tiny holes with a density of 100 holes per square centimetre. Concentration of holes in one direction is higher than in the other because metallic contacts for the base and the emitter are at the back side of the cell, placing the emitter contacts under the line of holes and the base contacts in the space between them (Figure 1). The holes have an original average diameter in the front side of 50µm and in the back side of 30µm. Finally, the wafers are etched for a second time to remove any possible damage generated by the drilling laser process (Cueto-Felgueroso [9]). This second bath removes approximately 5µm per face resulting in final diameters of the holes of 60µm and 40µm on the front and back side respectively and a thickness of approximately 190µm.
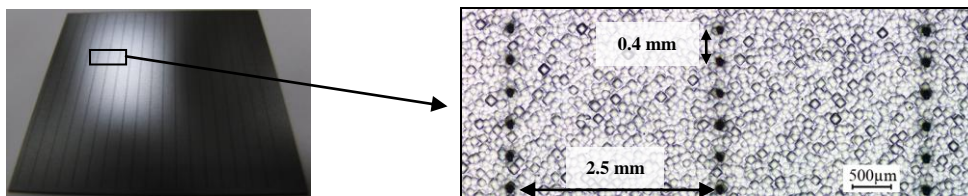
Figure 1: Sample of drilled wafer and zoom of the hole pattern

The second set of wafers serves as reference set. First, as with the other set of wafers, they have been chemical etched to remove any damage from wire-sawing and after that, they have been etched once again. This second etching process has been done to get a set as similar as possible to the set with holes, the only difference being the holes.

Wafers of both sets have been cut in 52.5mm x 52.5mm samples after the second chemical bath. The influence of any possible damage caused in this step can be neglected because the ring on ring test has been chosen for the study and failure in this type of test is usually caused by surface cracks or defects located at some distance from the wafer edges.

The raw material of the wafers is <100> mono-crystalline silicon grown by the Czochralski method. The crystal exhibits anisotropic behaviour being represented by means of the elastic constants $c_{11} = 165.6$ GPa, $c_{12} = 63.9$ GPa and $c_{44} = 79.5$ GPa.

3 Test description

The evaluation of the damage induced by the holes has been done employing the ring on ring test. In this test, the wafer is supported by a ring (20 mm of diameter) and the load is applied on the other side of the wafer by means of a ring of smaller diameter (10 mm). Figure 2 shows a photo of the test setup. Stresses inside the lower ring are much higher than in the outer part taking only into account the damage caused by the holes. Hence, influence of border cracks that might exist can be neglected.

The small thickness of the samples results in non-linear behaviour during the tests due to the large displacements. Figure 3 shows the test results of the study for both sets and the fracture load histograms where the strength and the scattering can be observed.
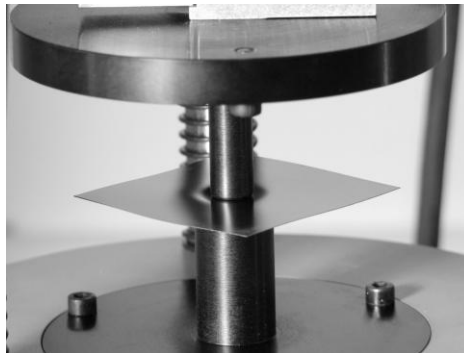
Figure 2: A photograph of the ring on ring test

4 Finite Element models

The test gives information about the behaviour of the samples and the maximum load and displacement reached before failure takes place. However, it's also necessary to determine the final stress at fracture. The finite element method has been used for the simulation to account for both the anisotropy of mono-crystalline silicon and the non-linear behaviour of the sample during the test. The non-linearities present in the test are due to large displacements and contact between the wafer and the rings. The software ANSYS has been used to develop a model in which wafer and supports have been modelled with shell elements, as recommended in Barredo [10]. The mesh is finer in the contact zone to avoid convergence problems (figure 4).
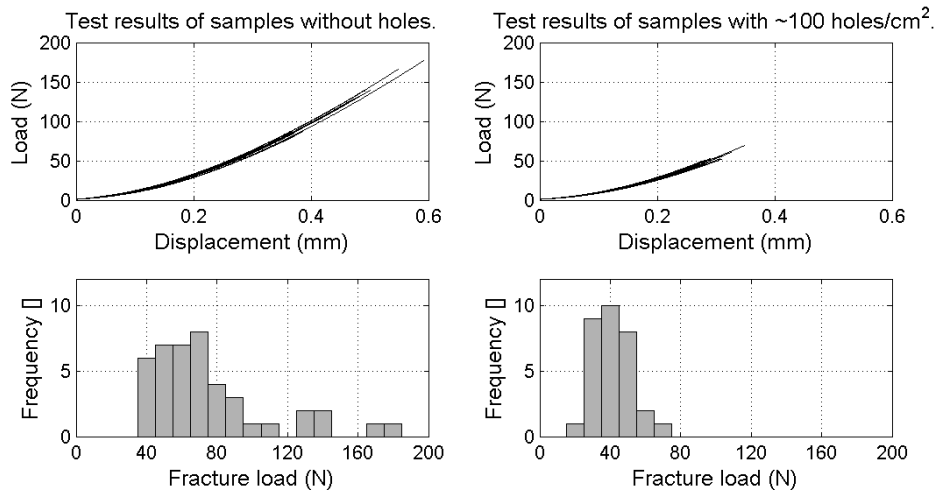
Figure 3: Load-displacement curves and fracture load histograms for both sets
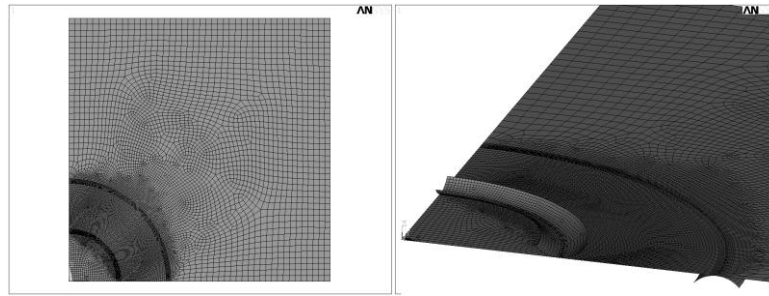
Figure 4: FE model mesh

5 Stress concentration factor

A stress concentration factor has been estimated for the drilled wafers subjected to a biaxial stress state. To this end, the test results for the set of drilled wafers have been simulated with models including the holes and models without them and the maximum stresses have been compared.

5.1 Models without holes

The analysis of the test results for models without holes has been carried out developing two finite element models: one corresponding to the thinnest sample of the set and one corresponding to the thickest. Figure 5 shows the correlation between the test results and the FE models. The maximum principal stress in the moment of failure for all samples has been obtained through a linear interpolation taking into account the elastic energy stored in the wafer before failure and its thickness.
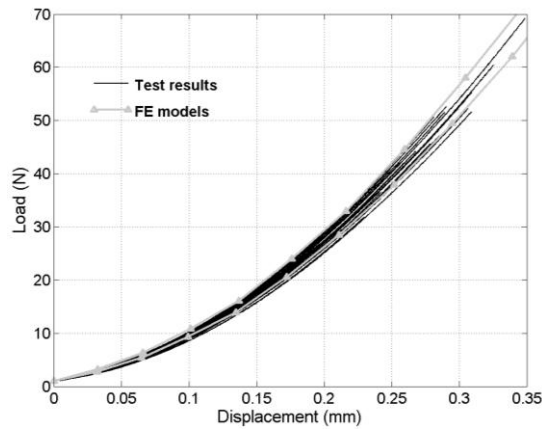
Figure 5: Test results and FE simulations for the set of drilled samples

5.2 Models with holes: Sub-models

The simulation of the stress concentration around the holes requires a very fine mesh which results in unacceptable calculation times. Hence, the sub-modeling technique also called cut boundary displacement method has been employed for this study. This method requires the development of a coarse model and the displacements calculated with this model are the boundary conditions for the sub-model. Therefore, a coarse FE model without holes has been developed as in the previous case. For this study, the mesh is created through a block with the dimensions of the sub-model so the displacements of the boundary of the block will be directly calculated to be imposed as boundary conditions to the sub-models. In figure 6 the coarse model without holes is presented marking the boundaries of the blocks. The test is simulated by means of the coarse model recording the displacement fields in the boundaries of all blocks for each load step. After that, so many sub-models as number of holes are developed imposing in each one the corresponding displacements of the boundary obtained with the coarse model. Finally, the stress field of each sub-model is calculated in the moment of failure getting the stress state of the whole sample including the stress concentration around the holes.

Previous to that, a mesh convergence study has been carried out for the sub-model. In figure 6, the coarse model and the mesh chosen for the sub-model are presented as well as the results of a mesh convergence study.
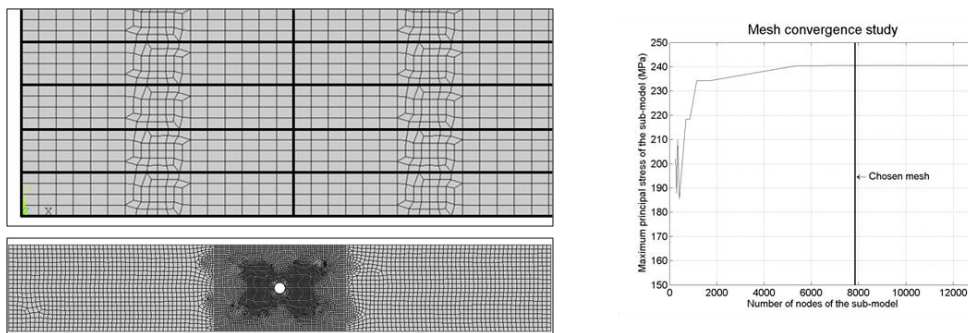
Figure 6: The coarse model, the mesh of the sub-model and the result of the mesh convergence study

As in the simulation of the test results with models without holes, two coarse FE models have been developed corresponding to the thinnest and the thickest samples of the set. The sub-modeling method has been applied to these two cases getting the stress field in all sub-models for each load step of both simulations. Finally, the stress field in the moment of failure of each sample has been obtained through a linear interpolation taking into account the elastic energy stored in the sample and the wafer thickness.

The stress concentration is a local effect which affects only a small area around each hole (figure 7). Therefore, there is not overlapping between adjacent holes which means that each sub-model is able to study the stress field around each hole.
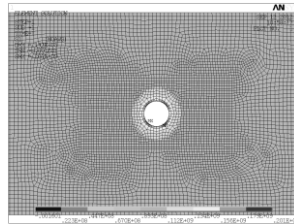
Figure 7: Stress distribution around a hole

5.3 The stress concentration factor

The first principal stress distribution in a ring on ring test simulation for the model without holes is presented in figure 8a. The analysis of the area subjected to a maximum stress (the one remarked in figure 8a) gives the following results: the mean value of the first principal stress is 618MPa, the standard deviation is 19.5MPa resulting in a coefficient of variation of 3.16%. Hence, it can be assumed that the first principal stress in the area analyzed has almost the same value. Figure 8b shows an enlarged view of the centre of the sample with the position of the holes. There are several holes inside the area of maximum principal stress so it can be expected that the maximum principal stress in the model with holes will be obtained at one of these holes. Therefore, the stress concentration factor has been obtained comparing the maximum principal stress of the model with holes with the model without holes, independent of the position where the maximum stress is achieved.
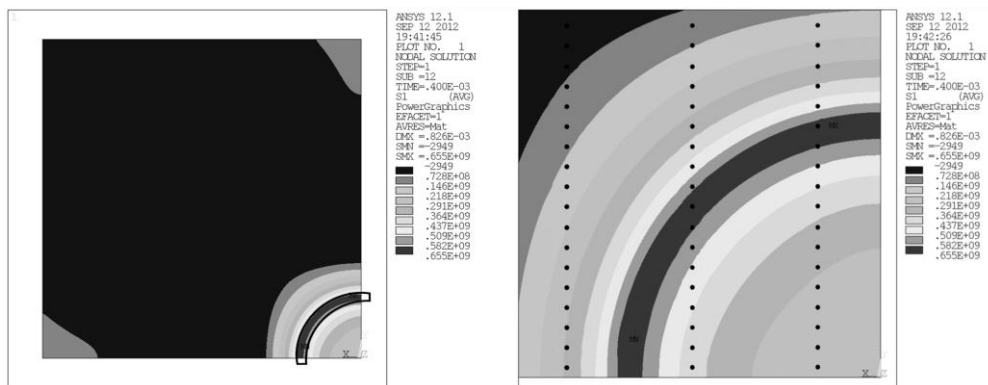
Figure 8: a) First principal stress distribution; b) Zoom of the centre with holes

In figure 9 the stress concentration factors calculated through the FE models are represented as well as the one proposed by Peterson [7] (K_t = 2.25) and the statistical values of the stress concentration factors calculated representing the range around the mean plus or minus one standard deviation (K_t = 2.22 ± 0.04). It can be seen that the values obtained are quite similar to the one taken from the literature validating the models with and without holes developed for the analysis of the test results.
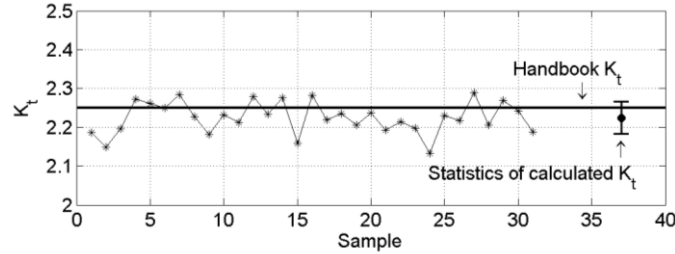
Figure 9: Stress concentration factors

6 Weibull analysis

The high scatter observed in the strength characterization of brittle materials is represented by means of statistical distributions getting a more accurate failure prediction. Based on the weakest link theory, Weibull [11] introduced a probabilistic approach in 1939 that is widely used in the strength characterization of brittle materials. This probabilistic model takes into account the so called size effect i.e. the influence of the size of the stressed edge, area or volume. As the failure initiates where the relation between the stress state and flaw or crack size and orientation is critical, an increase of the stressed edge, area or volume will reduce the strength because of the increased probability of having a weaker flaw. In this study only surface flaws are considered leading the failure so from now on the Weibull cumulative distribution function (cdf) will be described based on the area.

6.1 Development of the Weibull model.

The most general expression of the failure probability according to the Weibull model is given in eqn (1) which corresponds to the failure probability of a sample subjected to a uniform stress:

$$P_f(\sigma) = 1 - \exp\left(-\int_A \left(\frac{\sigma - \lambda}{\delta}\right)^\beta dA\right)$$

(1)

This is called the three-parameter Weibull cdf where the parameters define the failure of the material. The three parameters of the Weibull cdf have the following meaning:
   i) λ is the location parameter and it represents a threshold stress for which stresses below this value will never lead to the failure of the sample. It's given in MPa.
   ii) δ is the scale parameter. The sum of the scale and the location parameter gives the characteristic fracture stress which counts on the 63.2% of the samples with a unity area will fail. Its dimensions are [stress x (area)$^{1/\beta}$].
   iii) β is the shape parameter (dimensionless) and gives information about the scattering of the results. As β increases, the dispersion is reduced.

If $\lambda=0$, the cumulative distribution function is called the two-parameter Weibull cdf and it's also widely used in the strength characterization of brittle materials (Schoenfelder [3], Bagdahn [5], Borrero [12]).

For a material whose strength is characterized by a Weibull cdf with parameters λ, δ and β, the probability of failure of an infinitesimal area ΔA under uni-axial and uniform tension (σ) is calculated according to eqn (2). This is the most common way to find the Weibull cdf (especially if the two parameter Weibull distribution is employed i.e. $\lambda=0$).

$$P_{f,\Delta A}(\sigma) = 1 - \exp\left(-\Delta A\left(\frac{\sigma-\lambda}{\delta}\right)^{\beta}\right) = 1 - \exp\left(-\left(\frac{\sigma-\lambda}{\delta_\theta}\right)^{\beta}\right) \tag{2}$$

$\delta_\theta = \delta\,(\Delta A)^{-1/\beta}$ is the scale parameter for the area ΔA. It has stress dimensions and the addition to the location parameter results in the characteristic fracture stress (σ_θ) at which 63.2% of all samples of area ΔA will fail.

As has been mentioned, the expression shown in eqn (2) is valid for a uni-axial and uniformed tensioned area. This assumption is generally not true so it's necessary to obtain a valid expression for the test conditions in order to fit a Weibull cdf to the test results. In this case, the ring-on-ring test results in a non uniform biaxial stress distribution. To find the failure probability, the Principle of Independent Action (PIA) (Nemeth [13]) has been applied which is explained later. Now, the determination of the Weibull parameters is explained in more detail.

First of all, it's necessary to define the equivalent area A_{eq} as the area that subjected in a tensile test to the maximum stress observed in the sample in the moment of failure results in the same probability of failure. Therefore, the A_{eq} of the test i for the three-parameter Weibull cdf can be calculated as follows:

$$A_{eq} = \int_{dA|\sigma>\lambda} \left(\frac{\sigma_i-\lambda}{\sigma_{\max}-\lambda}\right)^{\beta} dA \tag{3}$$

The survival probability of the sample with area A and non uniform stress σ is equal to the survival probability of the equivalent area (A_{eq}) subjected to the maximum stress (σ_{max}) in the moment of failure. The equivalent area can be divided into n components of infinitesimal area ΔA (where the Weibull parameters of the material are known) subjected to σ_{max}. Finally, as the Weibull cdf is based on the weakest link theory, the survival probability of the equivalent area A_{eq} under σ_{max} is the same to the product of the survival probabilities of the infinitesimal areas ΔA subjected to σ_{max}.

$$P_{s,A}(\sigma) = P_{s,Aeq}(\sigma_{\max}) = \prod_i^n P_{s,\Delta A}(\sigma_{\max})_i = \left[P_{s,\Delta A}(\sigma_{\max})\right]^n = \left[P_{s,\Delta A}(\sigma_{\max})\right]^{Aeq/\Delta A} \tag{4}$$

Therefore, the probability of failure of a sample of a material with parameters λ, δ_θ and β (referred to an infinitesimal area ΔA) defining its strength and subjected to a uni-axial and non uniform stress field is:

$$P_{f,A}(\sigma) = 1 - \exp\left(-\frac{A_{eq}}{\Delta A}\left(\frac{\sigma-\lambda}{\delta_\theta}\right)^{\beta}\right) \tag{5}$$

The problem arises the other way round: the parameter defining the strength must be obtained from the data results. An iterative method to fit the test result to a three-parameter Weibull cdf, based on the one proposed by Przybilla et al [14], is next presented:

1. The failure stresses of the set analyzed (N samples) are sorted in ascending order. The probability of failure of the ith sample is:

$$P_{f,i,\exp} = \frac{i - 0.3}{N + 0.4} \tag{6}$$

2. The set of σ_i and $P_{f,i,exp}$ is fitted to a three-parameter Weibull cdf by the Least Square Method giving the experimental Weibull cdf.

3. The A_{eq} of each sample is calculated. The stress distribution obtained by means of FE analysis in combination with the parameters of the experimental Weibull distribution are used to evaluate the integral and to obtain the A_{eq} of each sample.

4. Knowing the equivalent area of each sample ($A_{eq,i}$), the probability of failure of this sample is calculated referred to ΔA by means of the following expression:

$$P_{f,i,\Delta A} = 1 - \left(1 - P_{f,i,\exp}\right)^{\Delta A / A_{eq,i}} \tag{6}$$

In this step, the procedure applied is different from the one proposed in Przybilla [14]. The equivalent area of samples without holes is almost four orders of magnitude higher than the one of the samples with holes. In order to fit results of both sets to the same ΔA and according to eqn (6), the failure probability will be so small or so high (depending on the set) that there may be convergence problems in the fitting of the three-parameter Weibull cdf to the σ_i, $P_{f,i,\Delta A}$ since all the values of $P_{f,i,\Delta A}$ will be very close to zero or very close to one. As the correlation factor is high ($R^2 = 0.98$), it's possible to use the values of the experimental Weibull cdf instead of the probabilities of failure obtained in eqn (5). Therefore, the eqn (6) may be transformed in eqn (7) giving a new set of data σ_i, $P^*_{f,i,\Delta A}$.

$$P^*_{f,i,\Delta A} = 1 - \exp\left(-\frac{\Delta A}{A_{eq}}\left(\frac{\sigma - \lambda_{\exp}}{\delta_{\theta,\exp}}\right)^{\beta_{\exp}}\right) \tag{7}$$

Eqn (7) permits to obtain new values of failure stress σ_i fixing the values of failure probability (eqn (8)) giving a new set of data $\sigma_{i,\Delta A}$, $P_{f,i,exp}$. This pair of data is composed by the original $P_{f,i,exp}$ and a new set of $\sigma_{i,\Delta A}$ which corresponds to the value of maximum stress which results in the same failure probability if the equivalent area is ΔA.

$$\sigma_{i,\Delta A} = \lambda_{\exp} + \delta_{\theta,\exp}\left[Ln\left(\frac{1}{\left(1 - P_{f,i,\exp}\right)^{A_{eq}/\Delta A}}\right)\right]^{1/\beta_{\exp}} \tag{8}$$

Using this expression has the great advantage of having values in the [0,1] range of failure probability making the adjustment to a three-parameter Weibull cdf by the Least Square Method easier.

5. The new set of data $\sigma_{i,\Delta A}$, $P_{f,i}$, ΔA are fitted to a new three-parameter Weibull cdf, giving three new parameters.

6. Going back to the third step, the iterative process continues till the variation of λ and δ is negligible.

This procedure is valid for an uni-axial stress field. For multi-axial stress, the Principle of Independent Action (PIA) has been applied. This model, proposed by Barnett (1967, [15]) and

Freudenthal (1968), states that the Weibull survival probability of a uniformly stressed material element under multi-axial loading is equal to the product of the survival probabilities for each of the tensile principal stresses applied individually (eqn (9)).

$$P_f(\sigma_1, \sigma_2, \sigma_3) = 1 - \exp\left(-\int_A \left[\left(\frac{\sigma_1 - \lambda}{\delta}\right)^\beta + \left(\frac{\sigma_2 - \lambda}{\delta}\right)^\beta + \left(\frac{\sigma_3 - \lambda}{\delta}\right)^\beta\right] dA\right) \tag{9}$$

The PIA model is included in the iterative procedure through the calculation of the equivalent area of each test by means of eqn (10).

$$A_{eq} = \int_{dA|\sigma_1,\sigma_2,\sigma_3>\lambda} \left[\left(\frac{\sigma_1 - \lambda}{\delta}\right)^\beta + \left(\frac{\sigma_2 - \lambda}{\delta}\right)^\beta + \left(\frac{\sigma_3 - \lambda}{\delta}\right)^\beta\right] dA \tag{10}$$

6.2 The stress concentration factor according to Weibull model

In section 5.3, the stress concentration factor around the holes for the drilled wafer was obtained through the relation of the maximum principal stress of each sample in the model without holes and the model with holes. The mean value of all samples was compared with the theoretical value found in the literature. Now, a new way to obtain the stress concentration factor is presented.

Assuming that the wafers strength is described by the Weibull probabilistic model, the adjustment of the experimental data to a Weibull cdf defines the strength of the set. As the set of drilled wafer has been analyzed by means of FE models with and without holes, its strength can be characterized considering that the wafers have holes or they haven't. The comparison of the Weibull parameters (figure 10) obtained in the fitting of the experimental data (steps 1 and 2 of the iterative process described in 6.1) may give a stress concentration factor.
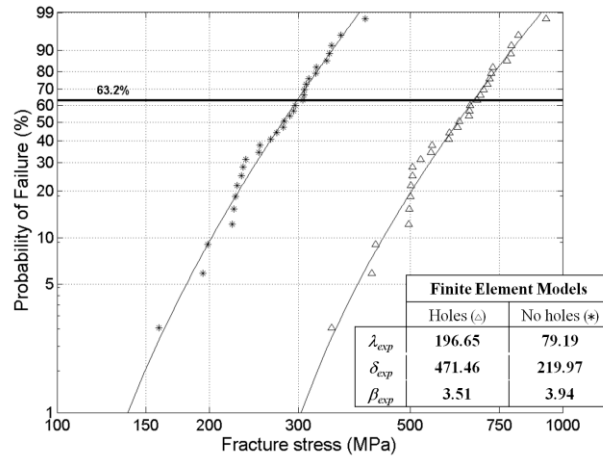
Figure 10: Weibull fitting comparison between model with or without holes

For material whose strength is described by the Weibull model, the characteristic fracture stress ($\sigma_{\theta,exp} = \lambda_{exp} + \delta_{exp}$) is employed to characterize the strength. Therefore, the stress concentration factor obtained is shown in eqn (11) resulting in a very close value to the ones obtained through the mean value comparison ($K_t = 2.22$) and according to Peterson ($K_t = 2.25$).

$$K_t = \frac{\sigma_{\theta,\exp,holes}}{\sigma_{\theta,\exp,no\,holes}} = \frac{[\lambda_{\exp} + \delta_{\exp}]_{holes}}{[\lambda_{\exp} + \delta_{\exp}]_{no\,holes}} = \frac{471.46 + 196.65}{219.97 + 79.19} = 2.23 \qquad (11)$$

6.2 Material properties

According to the iterative procedure described in 6.1, it's possible to obtain the parameters λ, δ_θ and β referred to an infinitesimal area ΔA which would completely define the strength of the material.

The equivalent area of each drilled wafer is very small since the maximum principal stress is very high because of the stress concentration factor. By definition, the equivalent area is the area subjected to the maximum stress resulting in the same probability of failure so, as the maximum stress is so high, the equivalent area is very small to equalize the failure probability. To obtain the material parameters, a $\Delta A = 40mm^2$ has been chosen which is much bigger than the equivalent area of the drilled wafer tests. Therefore, according to the iterative procedure explained in 6.1, the data set $[\sigma_i, P_{f,i,exp}]$ will move to the left till the convergence is achieved resulting in the final set $[\sigma_{i,\Delta A}, P_{f,i,exp}]$. The experimental fitting and the final one showing the material properties for a ΔA of $40mm^2$ is represented in figure 11.
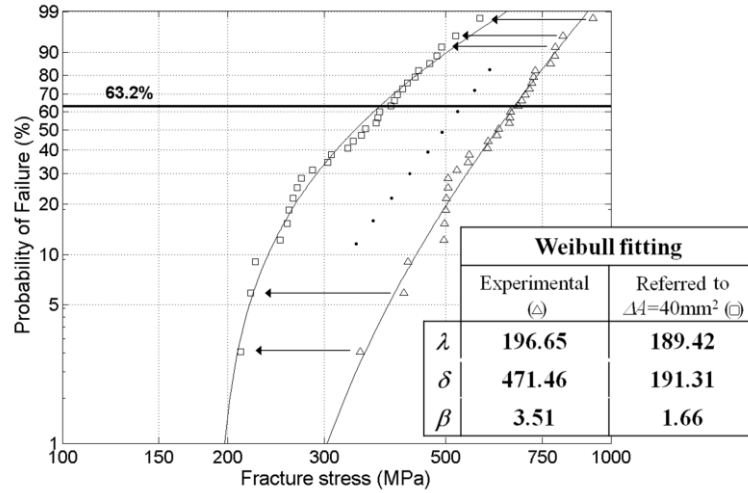
Figure 11: Experimental and final Weibull adjustment of drilled wafers

To validate the material parameters obtained with the drilled wafers, another set of wafers without holes and the same chemical treatment has been analyzed. In this case, the initial numerical model (without holes) is valid for the analysis due to the lack of holes.

In figure 12, the Weibull fittings of both sets are represented in logarithmic and linear scales. It can be seen that the location parameter (λ) is almost the same and there is a difference of 10% in the shape parameter (β). The scale parameter (δ_θ) presents a difference higher than the 30%.
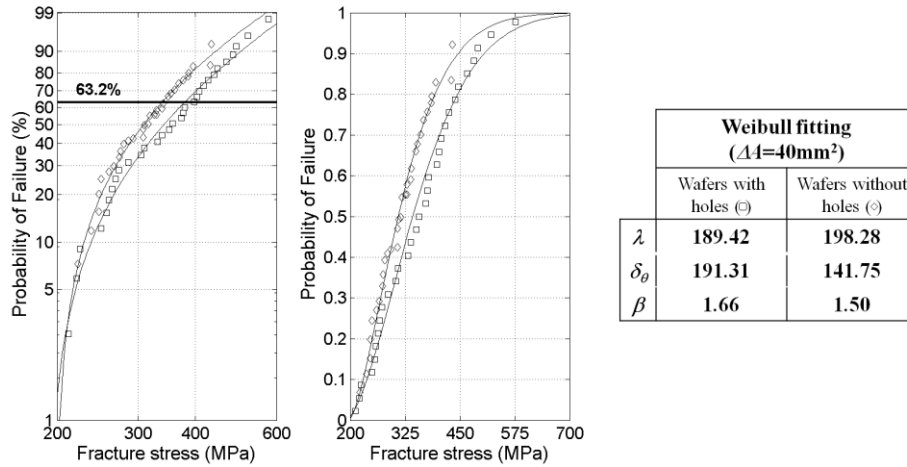
Figure12: Weibull fitting of wafer sets with and without holes

	Weibull fitting ($\varDelta A$=40mm²)	
	Wafers with holes (□)	Wafers without holes (◇)
λ	189.42	198.28
δ_θ	191.31	141.75
β	1.66	1.50

7 Discussion

The Weibull parameters defining the material strength have been obtained for two different set of wafers: one of them with thousands of tiny holes and the other one without holes. Results show that the location and shape parameter are quite similar while the scale parameter presents a bigger difference. Next some possible reasons justifying this are presented.

The drilling process involves a lot of variables which haven't been considered in this study. In figure 13 a hole viewed from the front side (a) and from the back side (b) is shown.
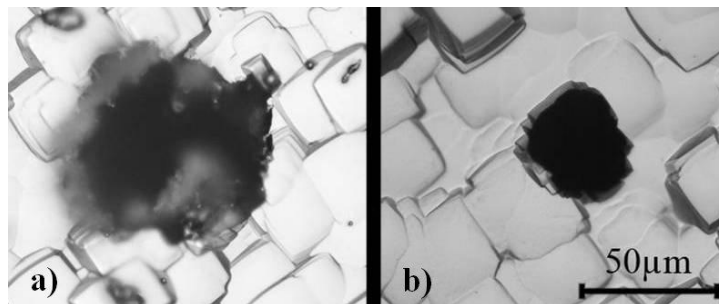
Figure13: a) Hole on the front, b) Hole on the back

First of all, the holes aren't perfectly round shape. Each hole presents a particular geometry more or less close to a round shape. However, small tips act also as stress concentrators. For the simulation all holes have been considered round.

Moreover, as it has been mentioned in section 2, the holes have bigger diameter in the front than in the back. In this case, holes have approximately a diameter of 60 μm in the front and 40 μm in the back. In the sub-models developed, the holes have been included with a diameter of 50 μm, as the average value of the two sides. However, if the failure is produced by tensile stress, it's more probable that it will start in the back surface. Therefore, it may be better to model the holes with a diameter of 40 μm.

The strength characterized via drilled samples is higher than the one obtained via normal samples. Hence, it seems that the hole diameter is playing an important role in the fracture process because if the model would have been developed with smaller holes, it is likely that the stress in the moment of failure would be lower and the Weibull parameters obtained with samples with holes would be closer to the ones obtained with normal samples.

8 Conclusions

The presence of holes in wafers prepared for EWT solar cells has an important influence in the mechanical strength. They act as stress concentrators leading the failure under lower stress state than in the case of no holes. A set of these drilled wafers has been analyzed to evaluate its influence in the failure of the samples.

To simulate the test by means of the Finite Element Method, the sub-modelling technique has been applied to avoid high calculation times. The simulation of one test with a model without holes takes more than 2 hours. The mesh convergence study establish the size of the mesh necessary to obtain accurate results so, the development of a model with this size of the mesh including 650 holes would require many computer resources and too much time to complete the simulation. The use of the sub-modelling technique is able from a computer resources point of view but the calculation times are also very high. One case has taken more than 30 hours to be completed.

The comparison of the maximum principal stress in the moment of failure of the drilled samples obtained by means of a FE models without holes with the ones obtained with models including the holes results in the stress concentration factors for each test. The mean value has been compared with the value proposed by Peterson giving close results. Moreover, another stress concentration factor has been obtained through the relation between the fittings of the test results to experimental Weibull cdfs giving a value with less than 1% of difference with the other two.

Finally, the material strength has been obtained from the drilled samples by means of a method described in detail. Results have been compared with the analysis of another set of reference wafers without holes resulting in very similar Weibull distributions. The main difference may be explained by the simplification of the real holes shape to a round shape and the difference between the modelled hole diameter (with the mean diameter of the hole lengthwise) with the real hole diameter on the back side of the wafer.

9 Acknowledgments

10 References

[1] Gee JM, Kumar P, Howarth J, Schroeder T, Franklin J, Dominguez J & Tanner D., Development of industrial high-efficiency back-contact Czochralski-silicon solar cells, *Progress in Photovoltaics: Research and Applications*, eds. John Wiley & Sons, Ltd., **19,** pp. 887–893. doi: 10.1002/pip.1075, 2011.

[2] Barredo J, Fraile A, del Rey I, Hermanns L., The influence of holes in the mechanical properties of EWT solar cells, *Proceedings of 11th International Conference on the Mechanical Behavior of Materials*, 2011.

[3] Schoenfelder S, Oswald M, Fischer C, Zühlke H-U, Berbig C, Geppert T, Wütherich T, Krokoszinski H-J, Bagdahn J., Investigations of Laser and Design Parameters of Via Holes on Mechanical Strength of Metal Wrap through Solar Cells, *Proceedings of the 25th European Photovoltaic Solar Energy Conference and Exhibition*, pp. 2578-2583, 2010.

[4] Cereceda E, Barredo J, Gutierrez JR, Jimeno JC., Mechanical Stability in Crystalline Silicon Solar Cells, *Proceedings of the 25th European Photovoltaic Solar Energy Conference and Exhibition*, pp. 1665 – 1668, 2010.

[5] Bagdahn J, Sharpe WH, Jadaan O., Fracture Strength of Polysilicon at Stress Concentrations, *Journal of Microelectromechanical Systems,* **12(3)**, pp. 302-312, 2003.

[6] Koepge R, Schoenfelder S, Giesen T, Fischmann C, Verl A, Bagdahn J. The Influence of Transport Operations on the Wafer Strength and Breakage Rate. *Proceedings of 26th European Photovoltaic Solar Energy Conference*, pp. 2072-2077, 2011.

[7] Peterson RE, *Stress Concentration Factors,* John Wiley & Sons, 1973.

[8] Barredo J, Hermanns L, Fraile A, Jimeno JC, Alarcón E., The influence of different surface treatments on the mechanical strength of silicon wafers. *Proceedings of 22nd European Photovoltaic Solar Energy Conference*, pp. 1164-1167, 2007.

[9] Cueto-Felgueroso G, Barredo J, Cereceda E, Hermanns L., Study of the mechanical strength improvement of wafers for EWT solar cells by chemical etching after the drilling process. *Proceedings of the 26th European Photovoltaic Solar Energy Conference*, pp. 1589 – 1592, 2011.

[10] Barredo J, Hermanns L, Del Rey I, Fraile A, Alarcón E. Comparison of Different FE Models for the Simulation of the Ring/Ball on Ring Test. *Proceedings of 10th International Conference on Computational Structures Technology*. Civil-Comp Press, Stirlingshire, UK, Paper 252, doi:10.4203/ccp.93.252, 2010.

[11] Weibull W. A Statistical Theory of the Strength of Materials. *Proceedings of the Royal Swedish Institute of Engineering Research*, **151**, 1939.

[12] Borrero-López O, Vodenitcharova T, Hoffman M, Leo AJ. Fracture Strength of Polycrystalline Silicon Wafers for the Photovoltaic Industry. *Journal of the American Ceramic Society*; **92**, pp. 2713-2717. doi: 10.1111/j.1551-2916.2009.03287.x, 2009.

[13] Nemeth NN, Powers LM, Janosik LA, Gyekenyesi P. CARES/LIFE Ceramics Reliability Evaluation of Structures Life Prediction Program. *National Aeronautics and Space Administration (NASA)*. Glenn Research Center. 2003.

[14] Przybilla C, Fernández-Canteli A, Castillo E. Deriving the primary cumulative distribution function of fracture stress for brittle materials from 3- and 4- point bending test. *Journal of the European Ceramic Society*, **31**, pp. 451-460, 2011.

[15] Barnett RL, Connors CL, Hermann PC & Wingfield JR., *Fracture of brittle materials under transient mechanical and thermal loading*, U.S Air Force Flight Dynamics Laboratory, AFFDL-TR-66-220, 1967.